

# Main upwelling regions in the Baltic Sea — a statistical analysis based on three-dimensional modelling

Kai Myrberg and Oleg Andrejev

*Finnish Institute of Marine Research, P.O. Box 33, FIN-00931 Helsinki, Finland  
(e-mail: kai.myrberg@fimr.fi)*

Myrberg, K. & Andrejev, O. 2003: Main upwelling regions in the Baltic Sea — a statistical analysis based on three-dimensional modelling. *Boreal Env. Res.* 8: 97–112. ISSN 1239-6095

In the Baltic Sea upwelling is an important process, especially in the coastal areas, causing vertical mixing and displacement of the water body. During thermal stratification, when the surface layer of the water is depleted of nutrients, upwelling plays a key role in replenishing the euphotic zone with the nutritional components necessary for biological productivity. Up to now, only a few comprehensive investigations have been carried out to study the locations of the main upwelling areas in the Baltic and how commonly these upwellings take place. Here, three-dimensional high-resolution modelling is used as a tool to statistically estimate an index reflecting the persistency of upwellings (downwellings) in various parts of the Baltic. This estimate is made for the summer season over the ten-year period from 1979 to 1988. The new idea in this paper is to use the persistency (stability) of the vertical velocity to define an upwelling index, instead of calculating the frequency of upwelling on the basis of changes in the sea-surface temperature, as is usually done. The model results were compared with measurements of surface temperature and salinity in the Gulf of Finland in 1988, where several strong upwelling cases were observed. The fit between the model results and measurements was found to be good. The upwelling indexes were compared with corresponding upwelling frequencies in the Swedish coastal area based on an analysis of long-term sea-surface temperature measurements. The results, based on these two different approaches, correspond well with each other. Consequently, we can expect that the three-dimensional model can be used to good effect as a tool to describe the overall statistics of the main upwelling areas in the Baltic. The results of the ten-year simulation show that coastal-type upwellings (downwellings) dominate, with values of the index as high as 30%–50% (–30% to –50%), being typically between 10% and 30% (–10% to –30%). The width scale of upwellings (perpendicular to the coast) is typically only 5–20 km. The length scale is somewhat more variable, being typically between 30 and 150 km (alongshore).

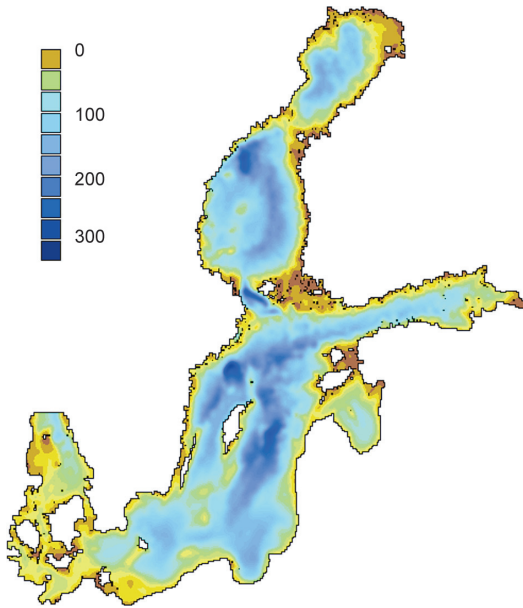


**Fig. 1.** The bottom topography of the Baltic Sea with corresponding sea depths in metres. The scale of the colours is shown in the palette.

## Introduction

The Baltic Sea (Fig. 1) is one of the largest brackish water areas in the world. It has a very limited water exchange with the open ocean via the narrow and shallow Danish Sounds and is characterized by a significant fresh-water surplus due to large river runoffs. This leads to a two-layer salinity stratification, which plays an important role in the basic physics. The currents in the Baltic Sea are mainly caused by wind stress, even though thermohaline effects cannot be disregarded. The sea-surface slope resulting from the permanent water supply due to river runoff contributes appreciably to the existing circulation pattern. The Baltic Sea is very shallow, having a mean depth of only 55 m. Thus, the bottom topography plays a role modifying the physical processes and, in spite of the comparatively small size of the sea, its various sub-basins have their own special hydrographic characteristics. The Baltic Sea has a meridional extent of about 650 km and a latitudinal extent of more than 1500 km. The complex physics of the sea and its relatively limited size make it a challenging marine environment, a “marine

laboratory”, which allows us to study different physical processes by using measurements with a relatively high spatial and temporal resolution. The measurements support model simulations by providing good verification material to test the models’ reliability in describing the physics of the sea.

One of the key physical features in the Baltic Sea is upwelling; coastal upwelling is usually the most important in such a semi-enclosed shallow sea, where the isopycnic levels are in many places rather close to the sea surface (Hela 1976, Nömmann *et al.* 1991). Upwelling is an important process in bringing nutrient-rich waters from deep layers to the surface, in mixing water masses and in generating frontal areas (Kahru *et al.* 1995). During an upwelling, the surface temperature can drop by about 10 degrees in a few days (Hela 1976). Upwellings can be significant in replenishing the surface layers with the nutritional components necessary for biological productivity (*see e.g.* Kononen and Niemi 1986, Raid 1989, Fonselius 1996). In spite of the important role of upwellings in the physics and biology of the Baltic Sea, only a rather limited number of papers have been devoted to studying it (*see next section*).

The main purpose of this study is to carry out a statistical analysis of upwellings in the Baltic Sea using a hydrodynamic model with a high spatial resolution and to get, for the first time, an overall statistical view of the main upwelling (downwelling) regions and correspondingly to define an upwelling index to show the persistency of upwellings (downwellings) in different areas. Those areas having a high persistency of upwelling can be expected to have high nutrient concentrations in the surface layers (brought from the layers below) and to be possibly correlated with enhanced biological activity. This study is focused on investigations of the uppermost layer of the sea. A new approach is to use a model-produced vertical velocity as the basis for the calculation of an upwelling index. This is because upwelling is practically defined as an area of rising water, and downwelling as the converse.

The model used here is a three-dimensional baroclinic hydrodynamic model (Andrejev and Sokolov 1989, Sokolov *et al.* 1997, Andrejev *et*

*al.* 2000, Engqvist and Andrejev 2002). Upwelling characteristics are simulated for summer, from May to September, which covers the period when the main upwellings with potential biological relevance take place. The simulation period is ten years, from 1979 to 1988; this is expected to be long enough to give a reliable statistical view of the main upwelling areas with their corresponding persistencies.

In the next section we shortly summarize our present knowledge of the upwelling dynamics of the Baltic Sea, as well as of the World Ocean in general, as background information for our further studies, where too will be described the implementation of the model, as well as the data sets and forcing functions which have been employed for the numerical experiments. The methods used for the analysis of the upwellings and the index describing the persistency, are also dealt with. The analysis of the results starts with a comparison of the model results with observations. This is followed by a detailed analysis of the upwelling statistics, after which the study is concluded with a summary and a review of some practical consequences of the investigation.

## **An upwelling event and its specific features in the Baltic Sea**

Upwelling means, in general terms, vertical displacement of deep waters towards the surface. In reality, upwelling up to the surface layer never takes place from depths greater than a few hundred metres. The primary requisite for an upwelling is that horizontal advection should transport the surface waters away from the upwelling area, in other words, there must be a divergence of currents (Hela 1976).

Upwelling is a common event all over the World Ocean, especially in coastal areas. A comprehensive analysis of upwellings in different parts of the World Ocean is given e.g. by Tomczak and Godfrey (1995). From among the many studies, we may mention the following recent investigations for different parts of the World Ocean. Kosnyrev *et al.* (1997) did numerical simulation of upwelling events in the Black Sea, finding that the interaction of the sea's rim current with the coastline and bottom topography

leads to the development of an upwelling event, even in the absence of wind forcing. Oke and Middleton (2000) studied, also using numerical modelling, topographically-induced upwellings off Eastern Australia, where a region of persistent high bottom stress played a key role in driving upwellings. Chant (2001) used measurements to construct a three-dimensional view of interaction between upwelling circulation and near-inertial motion on New Jersey's inner shelf, while Mesias *et al.* (2001) presented a modelling study involving the coast of Chile. Their results indicate the formation of an equatorward coastal jet during intense upwelling activity induced by the prevailing equatorward winds. Rao (2002) presented observational evidence of the alongshore variability in coastal upwelling along the central east coast of India in response to the wind stress field.

According to certain studies, upwellings in the Baltic Sea can be expected to take place for several reasons. According to Hela (1976) at least the following types of upwellings should be mentioned (in the Northern Hemisphere). Firstly, transversal Ekman upwelling, produced externally by a wind component blowing alongshore. As a result of this, coastal upwelling (the most common type) takes place with the coast on the left-hand side (looking downwind) and offshore upwelling occurs with the coast on the right-hand side. Secondly, geostrophic transversal upwelling (this type of upwelling is also a response to winds producing Ekman upwelling), produced internally by an alongshore current, with the upwelling appearing on the left side of the current. This mechanism is most probably coupled with the development of internal Kelvin waves (Walín 1972, Svansson 1975). Thirdly, coastal upwelling brought about externally by the stress of seaward winds in shallow waters (so-called "Leewirkung"). This type can be rather important in shallow coastal areas (Svansson 1975). The fourth type is connected with divergences in the surface current field. This can be caused by several mechanisms: these include inhomogeneity in the bottom topography and the effect of the curl of the wind stress. According to Fennel and Seifert (1995), the intensity of upwelling varies alongshore during upwelling-favourable winds. This is due to the generation of Kelvin waves

in response to an alongshore wind decaying in time. The downwelling signal propagated by the Kelvin waves then overcomes the local Ekman upwelling.

Only a few studies have been carried out to discover the main upwelling areas in the Baltic and to estimate the typical lifetime of an upwelling event. Bychkova and Victorov (1986) analysed available satellite data for 1980–1984 and found that, during the stratified period, 14 upwelling zones exist. However, these observed areas are coupled with various wind events, so the results do not represent real long-term mean conditions. According to Bychkova and Viktorov (1986) the lifetime of upwellings ranges from 0.5 to 10 days, the temperature gradient at the sea-surface reaches  $0.5\text{--}1\text{ }^{\circ}\text{C km}^{-1}$ , and the total temperature difference between the upwelled waters and the open sea ranges from 2 to  $10\text{ }^{\circ}\text{C}$ . Further analyses of the upwelling parameters in the Baltic have been carried out, e.g., by Bychkova *et al.* (1990), Rudolff and Strübing (1991), Horstmann (1983) and Siegel *et al.* (1994), based on satellite data. Gidhagen (1987), using satellite data for the summer period in 1981–1983, focused on Swedish coastal waters. He concluded that coastal upwelling is a common phenomenon along the western coast of the Baltic. In some favourable coastal areas, upwelling occurs between a quarter and a third of the time. The satellite data indicate that the horizontal scales of the coastal upwellings are of the order of 100 kilometres alongshore and 10–20 kilometres in the off-shore direction.

The dynamics behind the development of real upwellings in the Baltic have been studied by, e.g., Haapala (1994), carrying out investigations of upwellings in the Gulf of Finland near the Hanko Peninsula during 1987–1988 (*see* section: case study in the Gulf of Finland). It was found that a wind parallel to the coastline should have a duration of about 60 h and correspondingly a wind impulse of about  $4000\text{--}9000\text{ kg m}^{-1}\text{ s}^{-1}$  to cause an upwelling event when thermal stratification exists. The vertical velocity can reach values of  $3 \times 10^{-5}\text{ m s}^{-1}$  (Hela 1976). Kahru *et al.* (1995), for example, concluded that upwelling is a key factor in the generation of frontal areas. The upwelling filaments that emerge when the upwelling front along a coast

becomes unstable are a common feature, e.g., in the north-western Gulf of Finland and along the eastern coast of the Bothnian Sea. These filaments are found to be effective transporters of water and substances.

It can be concluded that upwelling is one of the most important mechanisms causing vertical mixing in the coastal areas of the Baltic (*see* e.g. Svansson 1975, Haapala 1994). During the summer season, when thermal stratification exists, the surface layer of the sea is depleted of nutrients; upwelling then plays an important role for the plankton communities by transporting nutrients from the deep layers to the euphotic zone, with major temperature variations taking place in the 5–10 kilometres broad coastal zone (*see* e.g. Walin 1972, Haapala 1994, Lehmann *et al.* 2002). Gradually, the nutrient-rich surface waters are spread to larger areas due to advection and horizontal diffusion, and thus upwellings seem to directly enhance the overall primary production (Nömmann *et al.* 1991, Fonselius 1996, Semovski *et al.* 1999) and have a significant influence upon the spatial distribution of pelagic organisms, too (Raid 1989).

The climatic variability of upwellings has been studied by Lehmann *et al.* (2002). They found, based on three-dimensional modelling, that the different phases of the NAO index (NAO = North Atlantic Oscillation) in winter result in major changes of horizontal transports in the deep basins of the Baltic and in upwellings along the coasts, as well as in the open sea-area. During positive NAO indexes, strong Ekman-currents are produced with increased up- and downwelling along the coast, whereas during negative NAO indexes Ekman drift and upwellings are strongly reduced.

## Model implementation

The numerical model, which was developed by Andrejev and Sokolov (1989, 1990), is time-dependent, free-surface, baroclinic and three-dimensional. Simplifications, in the form of the hydrostatic approximation, the incompressibility condition, a Laplacian closure hypothesis for sub-grid-scale turbulent mixing, and the traditional f-plane approximation, are made. It is furthermore

assumed that density variations only manifest themselves in the buoyancy terms; elsewhere the density is taken to be constant. The governing equations and the numerical methods employed are discussed here briefly; more information is presented in the Appendix. A comprehensive presentation of the main equations and numerical methods employed can be found in Andrejev *et al.* (2000). The model has been applied to several studies. Engqvist and Andrejev (2002) used a cascade framework modelling approach in order to study water exchange in the Stockholm Archipelago. Andrejev *et al.* (2002) investigated the major Baltic inflow of 1993 and found excellent agreement between the model results and measurements. Using a high-resolution version of the three-dimensional model, O. Andrejev *et al.* (unpubl. data) investigated the mean circulation and water exchange in the Gulf of Finland.

### Main parameters and assumptions

In order to apply the model, it is necessary to specify a number of quantities. The horizontal kinematic eddy diffusivity coefficient  $\mu$  is prescribed to be constant ( $50 \text{ m}^2 \text{ s}^{-1}$ ) for the Baltic Sea. The vertical eddy diffusivity coefficient  $\vartheta$  is taken to be dependent on the local velocity shear and buoyancy forces (Kochergin 1987):

$$\vartheta = (0.05h)^2 \sqrt{\left(\frac{\partial u}{\partial z}\right)^2 + \left(\frac{\partial v}{\partial z}\right)^2 - \frac{g}{\rho_0} \frac{\partial \rho}{\partial z}} \quad (1)$$

where  $u$  and  $v$  are the velocity components along the eastward- and northward-directed  $x$ - and  $y$ -axes, respectively. The  $z$ -axis is taken to point downwards,  $\rho$  is density,  $\rho_0$  is a reference density and the gravitational acceleration is denoted by  $g$ . The parameter  $h$  is assumed to be 2.5 m, which is equal to the thickness of the uppermost layer in the model (*see* next section).

The wind stress components (Niiler and Kraus 1977) take the form

$$\tau_x = \rho_a C_d W_x |\overline{W}|,$$

$$\tau_y = \rho_a C_d W_y |\overline{W}|,$$

where  $W$  is the wind velocity and  $\rho_a$  is the density of air. Following Bunker (1977), the drag

coefficient  $C_d$  at the sea-surface was formulated as

$$C_d = 0.0012(0.066|W| + 0.63) \quad (2)$$

A quadratic law was used for the bottom friction, where the drag coefficient  $C_d$  was prescribed as 0.0026 (Proudman 1953).

The heat transfer and radiation balance at the air-sea interface is, following Lane and Prandle (1996), taken to be

$$F_T = Q_s + k(T_a - T_s), \quad (3)$$

where  $Q_s$  is the effective mean solar radiation, that is approximated by a sinusoidal function of the time of year and latitude,  $T_a$  is the air temperature,  $T_s$  is the sea-surface temperature and  $k$  is an exchange coefficient. The latter is calculated by an empirical expression, related to the square of the wind speed and temperature, and takes into account both conduction and evaporation. For salinity, the flux  $F_s$  is to a lowest-order approximation set to zero, because the difference between precipitation and evaporation is not known accurately due to a lack of observations.  $F_s$  is usually estimated to be slightly positive in the Baltic, but there are large discrepancies between the published estimates (e.g. Ehlin 1981, HELCOM 1986, Omstedt *et al.* 1997).

Vertical convection has to be parameterised, since the model uses the hydrostatic approximation. The following heuristic algorithm is used: first a check is made of whether the water in a grid cell is stable relative to the water of the underlying cell. If not, the water of the unstable grid cell (or some part of it, cf. Sokolov *et al.* 1997) is moved into the lower cell and the same volume of water from the lower cell is displaced upwards and mixed with the upper-cell water. This procedure of water replacement proceeds cell by cell until the sinking volume finds itself in stable conditions and the water column is well-mixed in the vertical direction.

### Set-up of the numerical model experiments

The model was used to investigate the ten-year period from 1979 to 1988. Annually, the simula-

tion period was from May 1 to September 30. This period was chosen because the objective of this paper is to study upwellings having biological relevance. The initial temperature and salinity fields for the model were assembled using a data assimilation system due to Sokolov *et al.* (1997), which in turn is coupled to a Baltic environmental database (Wulff and Rahm 1991) and to the three-dimensional model employed here. To construct the initial fields for May 1 each year (the first month of the numerical experiment every year is May), temperature and salinity data from the database for all the months of April from 1979 to 1988 were averaged. The reason for this somewhat artificial choice is the insufficient amount of true data available for a single specific April month. The model run was initiated from a quiescent state. Carrying out the model simulations for only the summer period leads to a questioning of the level of accuracy of the initial conditions used every spring. We have used the best initial conditions available to us, and started the simulation at the beginning of May every year, when the stratification conditions are as simple as possible due to an absence of vertical temperature gradients. Additionally, our rather successful model verifications show that the model adapts quickly to the prevailing hydrographic conditions.

The open boundary of the model domain is placed in the Kattegat along latitude 57°35'N. The horizontal resolution of the model is two nautical miles, and the time step used in the simulations is one hour. For the bottom topography we used a standard bathymetry provided by Seifert and Kayser (1995). Since the vertical velocity is very sensitive to the bottom roughness, the bathymetry field was filtered using a Tukey cosine filter (Tukey 1977) to remove the random properties of the bathymetry.

The Baltic model comprises 18 levels in the vertical with a monotonically-increasing layer thickness towards the bottom. The depths of the layer interfaces are: 0 m, 2.5 m, 7.5 m, 12.5 m, 17.5 m, 22.5 m, 27.5 m, 35.0 m, 45.0 m, 55.0 m, 65.0 m, 75.0 m, 85.0 m, 95.0 m, 105.0 m, 137.5 m, 162.5 m, 187.5 m and the bottom.

The SMHI (SMHI = Swedish Meteorological and Hydrological Institute) gridded meteorological data is used for 1979–1988 with a temporal

resolution of three hours and a spatial resolution of one degree over the entire Baltic Sea area (K. Boqvist, SMHI, pers. comm.). Since the wind velocities in the data set represent geostrophic values, they must be extrapolated to the sea-surface. A standard method for this correction is to multiply the wind speed by a factor of 0.6 and deflect the wind direction 15° counter-clockwise (B. Gustafsson, pers. comm.). Since our purpose is to investigate the climatic distribution of the upwelling index, the long-term mean monthly river discharges (Bergström and Carlsson 1994) are used for the main rivers of the Baltic Sea, to which the contributions from smaller rivers are added.

### The upwelling index

The upwelling index is defined as:

$$I = \frac{\sum_{n=1}^N w_n}{\sum_{n=1}^N |w_n|} \times 100\% \quad (4)$$

where  $w$  is a vertical velocity and  $n$  (1... $N$ ) is the time step. The index is calculated at each time step.

The index reflects the persistency of the vertical current component. If the vertical current is directed upwards/downwards throughout the whole simulation period, the index is equal to 100%/–100%. The more variable the direction of the vertical currents, the closer the index is to 0%.

## Comparison of model results with experimental data

### Upwellings along the Swedish coast

A comparison with the analyses of Gidhagen (1987) is carried out in the Swedish coastal area. These data are practically the only ones available for which upwellings are statistically analysed based on observations. Gidhagen studied in situ data of sea-temperature (0–5 m depth) over the ten-year period of 1973–1982. This analysis is based on sea-surface maps (40 coastal stations, 25 ships) that were plotted every second day at

SMHI. The analysis was carried out only for measurements within a distance of 10 km from the coast. Upwelling was considered as occurring if an in situ measurement showed a temperature drop of at least 2 °C compared with earlier and/or surrounding measurements (*see* Gidgahen 1987 for details). We calculated the upwelling index using Eq. 4 for the corresponding areas (and correspondingly at the 2.5 m level) and months (July, August, September), even though our period of investigation differs somewhat from that of Gidgahen (1987) and even though the parameters used in our calculations are not the same. The results of the comparison are shown in Table 1.

According to both the measurements and the model results, the same stations are characterized by the highest (Trellebrog, Ystad, Ratan) and lowest (Fårö, Svenska Högarna, Husum) upwelling indexes (Table 1). Differences of about  $\pm 5\%$  are found typically, but that is evidently due to the different temporal resolution between the model results and the data. The measurements show that at some stations (Kalmarsund, Landsort, Husum, Almagrundet) there is a tendency for the upwelling index to increase from June to September. The model results show exactly the same trend, even though some single indexes differ from the measurements by about  $\pm 5\%$ . The largest differences between the model results and the measurements appear in September. This is most probably due to the high wind speeds (autumn cooling) and the related variability on short timescales, not described by the measurements.

### Case study in the Gulf of Finland

Haapala (1994) carried out continuous current, temperature and conductivity monitoring at three stations near the Hanko Peninsula, in the Gulf of Finland, during 1978–1988. The model results of surface temperature and salinity (at a depth of 5 m) were compared with Haapala's measurements in summer 1988 at the same depth at station P1 (59°50'N, 23°14'E). The period under investigation included several strong upwelling events. After 21 July the surface temperature dropped rapidly by about 10 degrees and the sur-

face salinity increased correspondingly by about 0.5 PSU. Another strong upwelling was observed during September 10–20 with a decrease in surface temperature of more than 5 degrees and a corresponding increase in surface salinity of about 0.5 PSU (for details *see* Haapala 1994). The model (Fig. 2) was usually able to reproduce these upwelling cases rather well, with corresponding rapid changes in surface temperature and salinity. It should be stressed that the measurements were only available for every second day (data redrawn from the publication by Haapala 1994), while the time step in the model was 1 hour, which explains why the model results include much more high-frequency variability than the observations.

### Main upwelling (downwelling) regions in the Baltic Sea

Due to the limited extent and shallowness of the Baltic Sea, most of the upwelling events can be expected to take place in the near-coastal zone. The prevailing south-westerly winds (*see e.g.* Miettus 1998) are expected to play a dominant role in determining the spatial distribution of upwelling areas. We are also interested to know how large the values of the upwelling index, i.e. the persistency of upwellings, can reach in favourable areas.

**Table 1.** Upwelling frequency as percentage of time (during 1973–1982) for some Swedish coastal sections (Gidgahen, 1987) in comparison to calculated upwelling indexes (in parentheses).

Coastal station	July	August	September
Trelleborg	28 (28)	22 (25)	10 (23)
Ystad	28 (21)	22 (22)	11 (11)
Ratan	27 (23)	25 (12)	30 (15)
Bjuröklubb	22 (5)	11 (8)	20 (14)
Karlshamn	18 (25)	23 (22)	20 (22)
Kuggören	16 (18)	16 (14)	27 (24)
Kalmarsund	15 (14)	13 (15)	37 (32)
Sundsvallsb.	7 (12)	6 (4)	18 (12)
Landsort	5 (7)	15 (14)	27 (27)
Husum	2 (7)	2 (2)	14 (10)
Almagrundet	2 (8)	6 (12)	24 (23)
Fårö	0 (4)	0 (2)	0 (5)
Sv. Högarna	0 (1)	0 (6)	0 (5)

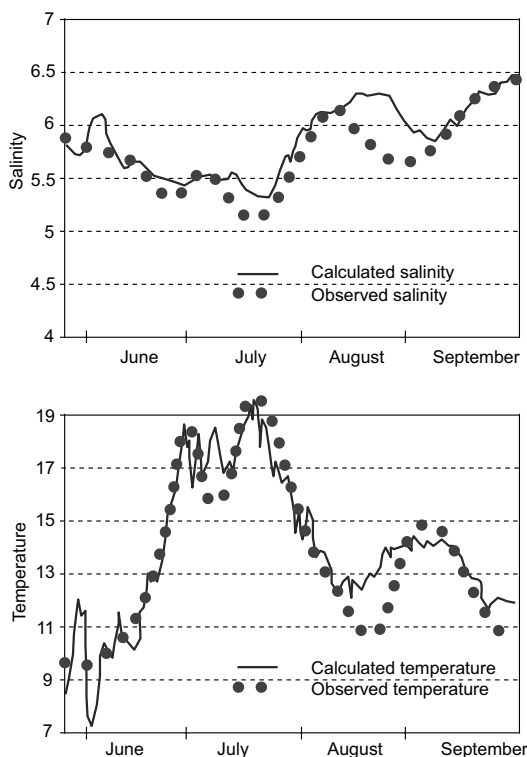


**Fig. 2.** Upper figure: the measured (dots) and simulated (unbroken line) surface salinity in PSU (at a depth of 5 m) near the Hanko Peninsula in the Gulf of Finland in June–September 1988 (measurements from Haapala 1994). Lower figure: the same as the upper one but for temperature (°C).

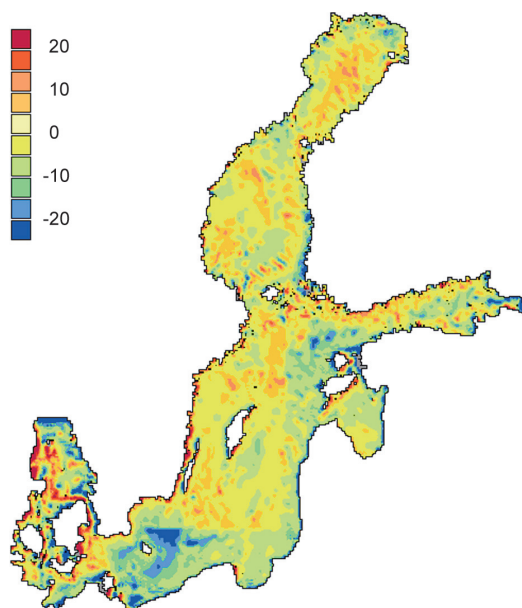


**Fig. 3.** Upwelling/downwelling index (percentage units) in the Baltic Sea (upwelling — positive values, downwelling — negative values). The scaling of the colours is shown in the palette.

For practical reasons, it is easiest to focus the study on the different sub-areas of the Baltic Sea separately and to investigate the upwelling index and reasons behind the resulting patterns

**Table 2.** Most important upwelling indexes in various sub-basins of the Baltic Sea with the corresponding length/width scales (U = upwelling, D = downwelling). \* = perpendicular to the coast, \*\* = alongshore.

Upwelling/downwelling area	Mean upwelling index (max/min) (%) (+ upwelling, – downwelling)	Width (km)*	Length (km)**
Bothnian Bay	10 (20) about –10	20	100
Eastern Bothnian Sea	–10 to –20 (–25)	5–20	100
North-western Baltic proper	10 (20)	20	70–90
Northern Gulf of Finland	10 to 20 (30)	10–25	150
Southern Gulf of Finland	–10 to –20 (–25)	5–15	200
Hiumaa	15 to 25 (30)/–15 to –25 (–30)	10–30 (U), 15–30 (D)	35 (U), 40 (D)
Saaremaa	15 to 25 (30)/–15 to –25 (–30)	10–45 (U), 5–40 (D)	100 (U), 75 (D)
Gotland	15 to 25 (30)/–10 to –20 (–25)	10–20 (U), 5–10 (D)	150
Western Baltic Proper	15–30 (40)	5–30	whole coast
Eastern Baltic Proper	–15 to –20 (–25)	5–10	whole coast
Southern Baltic	10 to –20 (–30)	5–10 (D), 300 (D)	45 (Gdansk)
(Polish and German coasts)	15 to 30 (40)	10 (U)	130 (Rügen)
Bornholm Island (B) and Bornholm Basin (BB)	20 to –30 /10 to 25 (B) –10 to –20 (BB)	10 (U, D) 85–350 (BB)	30(U), 20(D) 120 (BB)
Danish Straits	–30 to –50/40 to 60	10–30	10–100

in detail. The following figures represent the mean condition during the simulation period from 1979 to 1988 (May–September yearly). The investigation is concentrated on events at a depth of 2.5 m, which is expected to represent conditions in the uppermost layer of the sea with biological relevance. First the overall picture of the upwelling/downwelling areas for the entire Baltic Sea is presented, after which the sub-areas with pronounced features are further studied in more detail.

The result of the ten-years simulation for the entire Baltic is given in Fig. 3. It turns out that the main upwelling/downwelling areas are near the coasts (*see* detailed analysis below and Table 2), even though there are certain regions of the open sea-area, where the upwelling (downwelling) index can reach extreme values of between  $\pm 10$  and  $\pm 20\%$ . In coastal areas the main forcing function is the wind stress, but in open sea-areas the bottom topography and probably the curl of the wind stress play a role, too.

In the northern part of the Bay of Bothnia mostly weak downwellings take place (values around 10%), while in the middle part of the Bay upwellings take place, with indexes of between 10% and 20% (Fig. 3). This rather uneven upwelling area is due to the effects of bottom topography. The upwelling/downwelling pattern becomes visible in the Bothnian Sea, even if the structure is not so pronounced as in some other areas of the Baltic Sea. The mean wind conditions, with the dominance of south-westerly directions (*see* e.g. Launiainen and Laurila 1984), favour upwellings along the Swedish coast, while downwellings on average become visible along the Finnish coast. The upwelling area along the Swedish coast is rather uneven, but in some restricted areas indexes between 10% and 30% can be found. Some interesting upwelling patterns are situated in the southern Bothnian Sea, with an index of up to 20%; these are due to bottom topography. The lowest values of the index, representing downwellings, are about  $-25\%$  and typically between  $-10\%$  and  $-20\%$ , and are found along the Finnish coast (Fig. 4). This area has a length of about 150 km (alongshore) and a width of between 10 and 40 km. However, offshore of this near-coastal downwelling area a weak upwelling takes place. Thus,

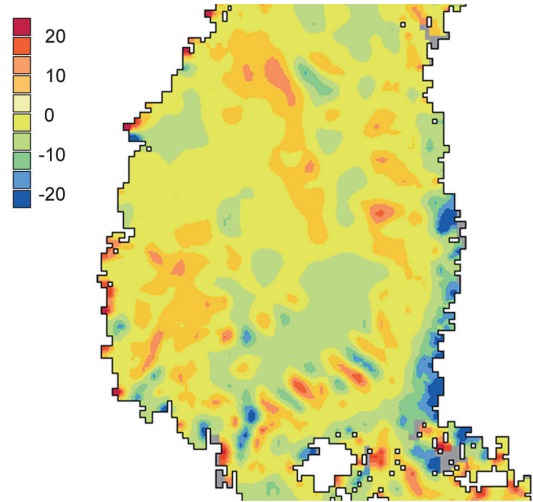


**Fig. 4.** Upwelling/downwelling index (percentage units) in the Bothnian Sea. Some linear features in the figure are due to the coarse resolution of the SMHI meteorological forcing even when data are interpolated to the sea model's grid.

a north–south oriented upwelling front along the length of the Bothnian Sea becomes visible even after the ten-years averaging procedure, the front thus being relatively persistent under various wind and thermal conditions. According to Kahru *et al.* (1995), this front (temperature) is known as the “Eastern Bothnian Sea Front”. The major mechanisms of the generation of such a front are: coastal upwelling complemented by coastal eddies, differential heating/cooling and water exchange between basins with different water characteristics.

In the Gulf of Finland, the predominantly south-westerly winds favour upwellings along the Finnish coast (Launiainen and Laurila 1984), where the largest values of the index are about 30% and typically between 10%–20% (Fig. 5). These upwellings on the Finnish coast, especially near the Hanko Peninsula, are well-known and well-documented (*see* e.g. Hela 1976, Bychkova and Viktorov 1986, Kononen and Niemi 1986, Haapala 1994, Kahru *et al.* 1995). The length of this upwelling area in the western gulf is about 150 km (alongshore) whereas the width scale is between 10 and 25 km. Upwellings also appear in the mouth areas of some of the major rivers of the gulf (Neva, Kymi, Narva, Luga) as well as in the eastern gulf to some extent. The southern

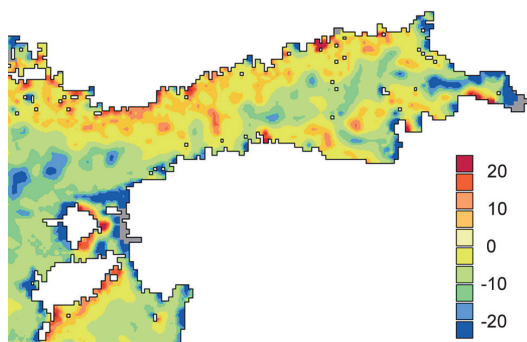


**Fig. 5.** Upwelling/downwelling index (percentage units) in the Gulf of Finland and around the islands of Hiiumaa and Saaremaa.

coast of the gulf is correspondingly characterized by downwellings. The lowest values of the index there are about  $-25\%$ , typically being between  $-10\%$  and  $-20\%$ . The length of this area, which partly covers areas west of the gulf, (with some gaps) is about 200 km and its width is ca. 5–15 km. In addition to the coastal upwelling/downwelling areas, a complicated mosaic-like structure of an upwelling/downwelling system is seen over the open sea area. This pattern is coupled with bottom topography and with the meso-scale circulation system (closed vortices) in the area (Table 2) studied by O. Andrejev *et al.* (unpubl. data).

The coasts of the Estonian islands of Hiiumaa and Saaremaa (Fig. 5) are characterized by a clear upwelling/downwelling system. The upwelling is intense, especially on the eastern coasts of Hiiumaa and Saaremaa, with a maximum index of about  $30\%$  and typical values of between  $15\%$  and  $25\%$ . On the west coast of both islands strong downwelling takes place, with a minimum index of about  $-30\%$  and typical values between  $-15\%$  and  $-25\%$  (Table 2). The dimensions of the upwelling/downwelling areas are: Hiiumaa — length 35 km, width 10–30 km/length 40 km, width 5–40 km; and for Saaremaa — length 100 km, width 10–45 km/length 75 km, width 5–40 km. The north-western Baltic Proper (Fig. 3) is characterised mostly by uneven upwelling areas having typical index values of  $10\%$ , sometimes up to  $20\%$ . These areas are again coupled with the bottom topography.

Another area with pronounced upwelling/downwelling systems is the surroundings of the

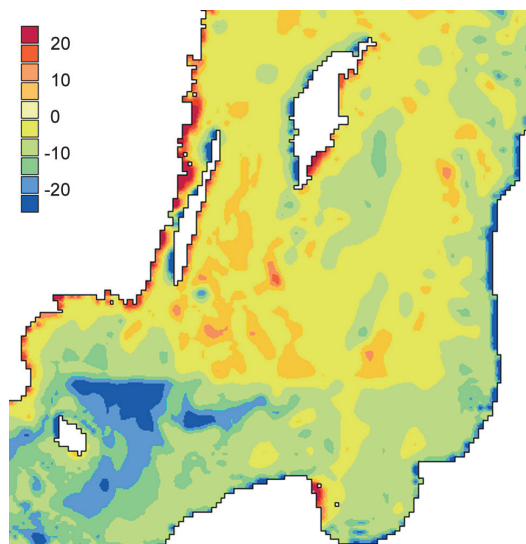


**Fig. 6.** Upwelling/downwelling index (percentage units) in the Baltic Proper (see caption of Fig. 4).

island of Gotland (Fig. 6). The predominantly south-westerly (Mietus 1998) winds cause upwellings to take place on average on the east coast of Gotland with a maximum index of about  $30\%$  and typical values between  $15\%$  and  $25\%$  (Table 2). The average condition on the western coast is just the opposite, with the prevailing south-westerly winds causing a downwelling there (minimum index of about  $-25\%$  and typical values between  $-10\%$  and  $-20\%$ ). The width of the upwelling zone is between 10 and 20 km and the length is about 150 km, while the width of the downwelling area is somewhat smaller, being 5–10 km; the length-scale also equals about 150 km. The situation is the same regarding the island of Öland. The upwelling/downwelling indexes are somewhat larger than in the case of Gotland.

The predominance of south-westerly winds and the related upwelling/downwelling patterns also become apparent when studying the east and west coasts of the Baltic Proper area: the west coast (Swedish coast) is characterized by upwellings, while along the eastern coast downwelling patterns dominate (Fig. 6). The maximum index for the upwellings is about  $40\%$ , with typical values between  $15\%$  and  $30\%$ , while the minimum value for the downwelling is  $-25\%$ , with corresponding typical values between  $-15\%$  and

–20% (Table 2). The upwelling/downwelling areas extend along the whole coast, with a width of 5–30 km on the western coast and 5–10 km on the eastern. An interesting general feature is that offshore of the coastal upwelling/downwelling areas, there is an opposite pattern (downwelling often takes place offshore of the coastal upwelling and vice versa); i.e. there exists a north-south-oriented front as found by Kahru *et al.* (1995) for temperature in the Bothnian Sea and in the Gulf of Finland.

The Polish coast (Fig. 6) is mostly a downwelling area (with typical values between –10% and –20% and a minimum of about –30%), because such a pattern is favoured by the prevailing south-westerly winds (Mietus 1998). On the western coast of the Gdansk Bay there is an upwelling region with maximum values of 40% and typical values between 15% and 30%; near the island of Rügen (Germany) there is also an upwelling area with values between 20% and 30%, occasionally 40%. The downwelling area has a width of 10 km and a length of 200 km (alongshore), while the upwelling areas have the following dimensions: Rügen — width 10–20 km, length 130 km; and the Gdansk Bay — width 10–20 km, length 45 km.

The surroundings of the island of Bornholm are also characterized by an upwelling/downwelling pattern with typical values of between 10% and 25% for upwellings and about –20% to –30% for downwellings (Fig. 6). The width of the upwelling region on the eastern coast is 10 km and the length-scale equals to 30 km, while for the downwelling area the corresponding values are 10 km and 20 km. A pronounced downwelling region exists in the Bornholm Basin with indexes between –10% and –20%. The dimensions of this region are: length 120 km (north–south), width 85–350 km (west–east). The easternmost part of this area is most probably connected with the overflow of water from the Bornholm Basin eastwards through the Stolpe channel towards the Gotland Deep (Table 2).

In the Danish Sounds area pronounced upwelling conditions are clearly visible. The whole east coast of Denmark is an upwelling area. However, because the model's open boundary is located near this area, a detailed

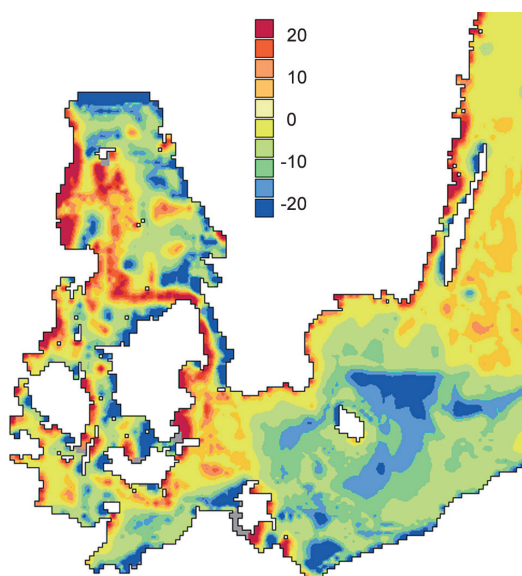


Fig. 7. Upwelling/downwelling index (percentage units) in the Danish Straits (see caption of Fig. 4).

analysis is omitted here. The Danish Sounds are characterised by a pronounced upwelling/downwelling system i.e. a frontal system exists there (Pedersen 1993). According to our simulations, the Danish side of the narrow Öresund is an upwelling area and the Swedish side a downwelling one. Similar structures are found correspondingly in the Great and Little Belt areas. The upwelling/downwelling structure is pronounced there; the upwelling index has a maximum of between 40% and 60%, while the minimum values in the downwelling regions are between –30% and –50% (Fig. 7 and Table 2). The width of the upwelling/downwellings is about 10–30 km while the length-scale varies considerably (ca. 10–100 km).

The rms of the upwelling index is presented in Fig. 8. The largest values of this parameter, indicating a pronounced dynamical activity, are naturally found in coastal areas where pronounced upwellings/downwellings take place. An especially interesting area is the Finnish coast in the Bothnian Sea as well as in the Bothnian Bay. In these locations, a north-south-oriented narrow band with very large values of rms up to 30% exists, which means that there is a pronounced variability in the upwelling/downwelling pattern. This area coincides with the area of active

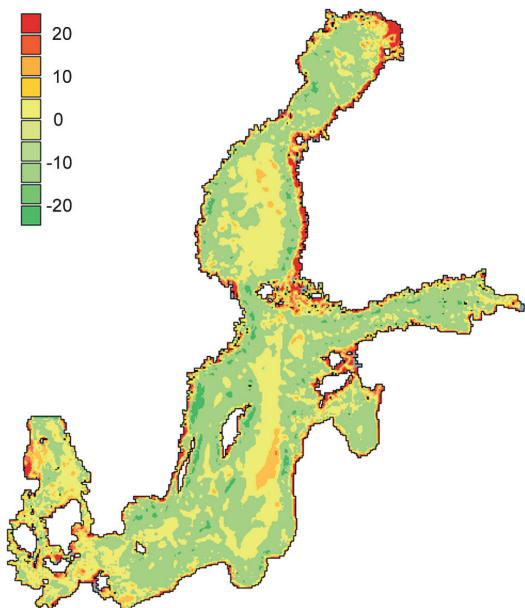


Fig. 8. The rms of the upwelling index.

frontal generation found by Kahru *et al.* (1995). High values of the rms of the upwelling index are found in Estonian coastal areas, including the Islands of Hiiumaa and Saaremaa, as well as in the Gotland Deep area, on the Polish coast and in the Danish Sounds. Maximum values are between 15% and 25% occur in these areas.

## Discussion and conclusions

Up to now, the sea-surface temperature and its spatio-temporal variations have been used as indicators for upwellings. However, in this paper we chose the model-derived vertical velocity and its related upwelling index to be the key parameter. This is because upwelling events are always, by definition, connected with upward-directed vertical velocities. Additionally, with the present model, it is possible to calculate the vertical velocity fields with a high spatial and temporal resolution.

Our study started with a comparison of our upwelling index values with corresponding upwelling frequencies in the Swedish coastal area analysed by Gidhagen (1987). There was a good fit between the results, even if our studies were based on different key parameters for

estimating the upwellings. It is encouraging for our future work that this comparison gave good results. It should also be remembered that the periods under investigation were not exactly the same. The comparisons of the model results with observations of strong upwellings in the Gulf of Finland in 1988 (Haapala 1994) gave encouraging results, too. The model could reproduce rather well the observed rapid and abrupt changes in surface temperature and salinity. Consequently, we may expect that the three-dimensional model can be successfully used as a tool to describe the overall statistics of the main upwelling areas in the Baltic, which was the main motivation of our study.

A statistical analysis for a ten-year period (May–September yearly) was carried out to calculate an upwelling index for the Baltic (in percentages) and to find out which areas are characterized by frequent upwellings (downwellings). The present approach to derive the index (Eq. 4) gives the same weight in the averaging procedure to each of the single index values  $I_n$  (calculated at each time step). However, it is possible to set a lower limit for vertical velocity and only to take into account values larger than that in the statistics. Vertical currents at the near-surface level (at 2.5 m) have been used, since the idea of this study was to investigate upwellings with biological relevance. We have studied the index at lower levels, too, but in the well-mixed layer (down to 15 m) there are no major differences to be reported compared with the 2.5 m level. Another reason for studying the 2.5 m level is that the coastal areas in some parts of the Baltic are very shallow, and we wanted to include the coastal areas with the most pronounced upwellings in our analysis. Our choice of model level also corresponds to that chosen by Gidgahen (1987).

The statistical analysis showed that the most persistent upwellings are those in coastal areas, even if it is difficult to verify this with observations. There is also naturally a clear correlation between the predominant climatological wind direction (south-west) and the locations of coastal upwellings. Open sea upwellings also occur, and in such cases the upwellings are additionally caused by the favourable shape of the bottom topography and/or are due to the curl of

the wind stress. It can be concluded that the main areas of coastal upwellings in the Baltic Sea are: the west coast of the Bothnian Sea, the northern coast of the Gulf of Finland, the west coast of the Baltic Proper, the east coast of Gotland, the east coasts of the Estonian islands, the east coast of Denmark including the Straits and areas east of the island of Bornholm. Typical index values are 10%–30% for both up- and downwellings. The width scale is typically 5–20 km (perpendicular to the coast), which is in accordance with the statement of Walin (1972) that major temperature variations take place in a 5–10 kilometres broad coastal zone. The length-scale is somewhat more variable, being typically between 30 and 150 km (alongshore).

It should be borne in mind that our aim is, based on a statistical approach, to discover the areas where upwelling/downwelling conditions prevail. Over shorter periods the existing upwelling/downwelling system can naturally be very different from the ten-year statistical mean conditions. Additionally, it should be pointed out that according to the definition of the index, downwellings can to some extent compensate upwelling events.

It should be realized that the main upwelling areas, with nutrient-rich waters entering the surface layer, are not exactly the same as those coupled with enhanced biological activity (like algae blooms, etc.) because sea currents transport and mix the water masses continuously. Thus the nutrient-rich, upwelled water masses may move away from the location where the upwelling originally took place.

It appears that in some areas there exists a clear upwelling-downwelling structure perpendicular to the coast. This means that if an upwelling zone exists in the coastal area, just offshore of it a corresponding downwelling zone becomes visible, and vice versa (e.g. in the Bothnian Sea). This is also reflected as a high rms of the upwelling index there. This structure has a close resemblance to the north–south oriented temperature fronts found by Kahru *et al.* (1995). According to Kahru *et al.* (1995) upwelling is one of the major mechanisms for the generation of such a front, although the part played by coastal eddies, differential heating/cooling, and water exchange between basins with different water

characteristics may also be important. Thus, the upwellings play an important role in the general dynamics of the Baltic Sea as well as in frontal development, and they determine areas where enhanced biological activity takes place.

## References

- Andrejev O. & Sokolov A. [Андреев О. & Соколов А.] 1989. [Numerical modelling of the water dynamics and passive pollutant transport in the Neva inlet]. *Meteorology and Hydrology* 12: 75–85. [In Russian].
- Andrejev O. & Sokolov A. 1990. 3D baroclinic hydrodynamic model and its applications to Skagerrak circulation modelling. In: *CBO 17th Conference of the Baltic Oceanographers Norrköping, Sweden*, pp. 38–46.
- Andrejev O., Myrberg K., Andrejev A. & Perttilä M. 2000. Hydrodynamic and chemical modelling of the Baltic Sea — a three-dimensional modelling approach. *Meri* 42, Report series of The Finnish Institute of Marine Institute, Helsinki, 41 pp.
- Andrejev O., Myrberg K., Mälkki P. & Perttilä M. 2002. Three-dimensional modelling of the main Baltic inflow in 1993. *Environmental and Chemical Physics* 24: 156–161.
- Bergström S. & Carlsson B. 1994. River runoff to the Baltic Sea: 1950–1970. *Ambio* 23: 280–287.
- Blumberg A. & Mellor G. 1987. A description of a three-dimensional coastal ocean circulation model. *Coastal and Estuarine Science Series* 4: 1–16.
- Bunker J. 1977. Computations of surface energy flux and annual air-sea interaction cycle of the North Atlantic. *Mon. Wea. Rev.* 105: 33–65.
- Bychkova I. & Viktorov S. 1986. Use of satellite data for identification and classification of upwelling in the Baltic Sea. *Oceanology* 27: 158–162.
- Bychkova I., Viktorov S., Demina M., Lobanov V., Losinsky V., Smirnov V., Smolyanitsky V. & Sukhaecheva L. 1990. Experimental satellite monitoring of the Baltic Sea in the 1980's. *ICES, C.M.* 1990/C:14.
- Chant R. 2001. Evolution of near-inertial waves during an upwelling event on the New Jersey inner shelf. *J. Phys. Oceanogr.* 31: 746–764.
- Ehlin U. 1981. Hydrology of the Baltic Sea. In: Voipio A. (ed.), *The Baltic Sea*, Elsevier Oceanography Series, Amsterdam, pp. 123–134.
- Engqvist A. & Andrejev O. 2002. Water exchange of the Stockholm Archipelago — a cascade framework modelling approach. *J. Sea. Res.* [In press].
- Fennel W. & Seifert T. 1995. Kelvin wave controlled upwelling in the western Baltic. *J. Marine System* 6: 289–300.
- Fonselius S. 1996. The upwelling of nutrients in the central Skagerrak. *Deep-Sea Res.* II 43: 57–71.
- Gidhagen L. 1987. Coastal upwelling in the Baltic Sea. Satellite and in situ measurements of sea-surface temperature indicating coastal upwelling. *Est. Coast. Shelf Sci.* 24: 449–462.

- Haapala J. 1994. Upwelling and its influence on nutrient concentration in the coastal area of the Hanko Peninsula, entrance of the Gulf of Finland. *Est. Coast. Shelf Sci.* 38: 507–521.
- Hela I. 1976. Vertical velocity of the upwelling in the sea. *Soc. Scient. Fennica. Commentat. Phys.-Math* 46: 9–24.
- HELCOM 1986. Water balance of the Baltic Sea. *Baltic Sea Environment Proceedings*, 16, Helsinki, Finland.
- Horstmann U. 1983. Distribution patterns of temperature and water colour in the Baltic Sea as recorded in satellite images: Indicators for phytoplankton growth. *Berichte aus dem Institute für Meereskunde and der Universität Kiel* 106, 147 pp.
- Kahru M., Håkansson B. & Rud O. 1995. Distributions of the sea-surface temperature fronts in the Baltic Sea as derived from satellite imagery. *Cont. Shelf Res.* 15: 663–679.
- Kochergin V. 1987. Three-dimensional prognostic models. In: Heaps N.S. (ed.), *Three-dimensional coastal ocean models, Coastal Estuarine Science Series 4*, American Geophysical Union, pp. 201–208.
- Kononen K. & Niemi Å. 1986. Variation in phytoplankton and hydrography in the outer archipelago. *Finnish Mar. Res.* 253: 35–51.
- Kosnyrev V., Mikhailova E. & Stanichny S. 1997. Upwelling in the Black Sea by the results of numerical experiments and satellite data. *Phys. Oceanogr.* 8: 329–340.
- Lane A. & Prandle D. 1996. Inter-annual variability in the temperature of the North Sea. *Cont. Shelf Res.* 16: 1489–1507.
- Launiainen J. & Laurila T. 1984. Marine wind characteristics in the northern Baltic Sea. *Finnish Mar. Res.* 250: 52–86.
- Lehmann A., Krauss W. & Hinrichsen H.-H. 2002. Effects of remote and local atmospheric forcing on circulation and upwelling in the Baltic Sea. *Tellus* 54A: 299–316.
- Liu S.-K. & Leendertse J. 1978. Multidimensional numerical modelling of estuaries and coastal seas. *Adv. Hydroscl.* 11: 95–164.
- Mesias J., Matano R. & Sturb P. 2001. A numerical study of the upwelling circulation off central Chile. *J. Geophys. Res.* 106: 19611–19623.
- Mesinger F. & Arakawa A. 1976. Numerical methods used in atmospheric models. *GARP publications series* 17, I, 64 pp.
- Mietus M. 1998. The climate of the Baltic Sea basin. *Marine meteorology and related oceanographic activities Report* 41, WMO/TD 933, Geneva, 64 pp.
- Millero F. & Kremling I. 1976. The densities of the Baltic Sea deep waters. *Deep Sea Res.* 23: 611–622.
- Niiler P. & Kraus E. 1977. One-dimensional models of the upper ocean. In: Kraus E. (ed.), *Modelling and prediction of the upper layers of the ocean*, Pergamon Press, Oxford, pp. 143–172.
- Nömmann S., Sildam J., Nöges T. & Kahru M. 1991. Plankton distribution during a coastal upwelling event off Hiiumaa, Baltic Sea: impact of short-term flow field variability. *Cont. Shelf Res.* 11: 95–108.
- Oke P.R. & Middleton J.H. 2000. Topographically induced upwelling off Eastern Australia. *J. Phys. Oceanogr.* 30: 512–531.
- Omstedt A., Meuller L. & Nyberg L. 1997. Interannual, seasonal and regional variations of precipitation and evaporation over the Baltic Sea. *Ambio* 26: 484–492.
- Orlanski I. 1976. A simple boundary condition for unbounded hyperbolic flows. *J. Comp. Phys.* 21: 251–269.
- Pedersen F. 1993. Fronts in the Kattegat: The hydrodynamic regulating factor for biology. *Estuaries* 16: 104–112.
- Proudman J. 1953. *Dynamical oceanography*. Methuen & Co., London, 409 pp.
- Raid T. 1989. The influence of hydrodynamic conditions on the spatial distribution of young fish and their prey organisms. *Rapp. P.-v. Réun. Cons. Int. Explor. Mer* 190: 166–172.
- Rao Narasimha T.V. 2002. Spatial distribution of upwelling off the central east coast of India. *Est. Coast. Shelf Sci.* 54: 141–156.
- Rudolff R. & Strübing K. 1991. Application of satellite remote sensing by the German federal Maritime and Hydrographic Agency. *GeoJournal* 24: 49–52.
- Seifert T. & Kayser B. 1995. A high resolution spherical grid topography of the Baltic Sea. *Meereswissenschaftliche Berichte* 9, Institute für Ostseeforschung, Warnemünde.
- Semovski S., Dowell M., Hapter R., Szczucka J., Beszczyńska-Möller A. & Darecki M. 1999. The integration of remotely sensed, seartruth and modeled data in the investigation of mesoscale features in the Baltic coastal phytoplankton field. *International Journal of Remote Sensing* 20: 1265–1287.
- Siegel H., Gerth M., Rudolff R. & Tschersich G. 1994. Dynamic features in the western Baltic Sea investigated using NOAA-AVHRR data. *Dt. Hydrogr. Z.* 46: 191–209.
- Simons T.J. 1974. Verification of numerical models of Lake Ontario. Part I: Circulation in spring and early summer. *J. Phys. Oceanogr.* 4: 507–523.
- Sokolov A., Andrejev O., Wulff F. & Rodriguez Medina M. 1997. The data assimilation system for data analysis in the Baltic Sea. *System Ecology contributions* 3, Stockholm University, Sweden, 66 pp.
- Svansson A. 1975. Interaction between the coastal zone and the open sea. *Finnish Mar. Res.* 239: 11–28.
- Tomczak M. & Godfrey J. 1995. *Regional oceanography: an introduction*. Pergamon Press, London, 422 pp.
- Tukey J.W. 1977. *Exploratory data analysis*. Addison-Wesley, Reading, Mass. xvi + 688 pp.
- Walin G. 1972. Some observations of temperature fluctuations in the coastal region of the Baltic. *Tellus* 24: 187–198.
- Wulff F. & Rahm L. 1991. A database and its tools. Wulff F. (ed.), *Large-scale environmental effects and ecological processes in the Baltic Sea. Research programme for the period 1990–95 and background documents*. SNV Report 3856, pp. 217–225.

## Appendix

In the model the governing equations are:

$$\frac{\partial u}{\partial t} + \frac{\partial uu}{\partial x} + \frac{\partial uv}{\partial y} + \frac{\partial uw}{\partial z} = -fv - \frac{1}{\rho_0} \frac{\partial p}{\partial x} + \mu \Delta u + \frac{\partial}{\partial z} \left( \vartheta \frac{\partial u}{\partial z} \right), \quad (\text{A1})$$

$$\frac{\partial v}{\partial t} + \frac{\partial vu}{\partial x} + \frac{\partial vv}{\partial y} + \frac{\partial vw}{\partial z} = -fu - \frac{1}{\rho_0} \frac{\partial p}{\partial y} + \mu \Delta v + \frac{\partial}{\partial z} \left( \vartheta \frac{\partial v}{\partial z} \right). \quad (\text{A2})$$

$$\frac{\partial u}{\partial x} + \frac{\partial v}{\partial y} + \frac{\partial w}{\partial z} = 0, \quad (\text{A3})$$

$$\rho = \rho(T, S) \quad (\text{A4})$$

$$\frac{\partial \rho}{\partial z} = \rho g, \quad (\text{A5})$$

$$\frac{\partial A}{\partial t} + \frac{\partial uA}{\partial x} + \frac{\partial vA}{\partial y} + \frac{\partial wA}{\partial z} = \mu_\lambda \Delta A + \frac{\partial}{\partial z} \left( \vartheta_\lambda \frac{\partial A}{\partial z} \right) + F_\lambda. \quad (\text{A6})$$

Equations A1 and A2 describe the momentum balances for the velocities  $u$  and  $v$  in the  $x$  and  $y$  directions respectively, where  $x$  increases eastwards and  $y$  increases northwards. The velocity along the downward-directed  $z$ -axis is denoted by  $w$ , pressure by  $p$ , and  $\rho_0$  is a reference density. Equation A3 is the volume conservation equation, where the small compressibility of water is neglected (hereby introducing a negligible mass conservation error). The equation of state A4 thus also reflects the absence of depth dependence (Millero and Kremling 1976).

Equation A5 takes into account the vertical density variations, which are not reflected in Eqs. A1 and A2. This is often referred to as the Boussinesqian hydrostatic approximation. The gravitational acceleration is  $g$ , and in Eq. A6  $A$  denotes the concentration of the modelled scalar properties that transgress the model boundaries or have sources/sinks (denoted  $F_\lambda$ ), within the model domain. These scalars are salinity  $S$  and heat  $\rho C_p T$  (where  $C_p$  is the specific heat of water and  $T$  is the temperature).

The kinematic eddy diffusivity coefficients in the horizontal and vertical directions are  $\mu$  and  $\vartheta$ , respectively, the Coriolis parameter is  $f$ , and the horizontal Laplacian operator is denoted by  $\Delta$ . External forces, such as wind stress and bottom friction, enter as boundary conditions. For the sea-surface  $z = -\zeta(x, y, t)$  these are:

$$\vartheta \frac{\partial u}{\partial z} = \frac{-\tau_x}{\rho_0}, \quad (\text{A7})$$

$$\vartheta \frac{\partial v}{\partial z} = \frac{-\tau_y}{\rho_0}, \quad (\text{A8})$$

$$\vartheta_\tau \frac{\partial T}{\partial z} = -q_\tau, \quad (\text{A9})$$

$$\vartheta_s \frac{\partial u}{\partial z} = -q_s, \quad (\text{A10})$$

$$p = p_a \quad (\text{A11})$$

$$w = \frac{\partial \zeta}{\partial t} + u \frac{\partial \zeta}{\partial x} + v \frac{\partial \zeta}{\partial y}, \quad (\text{A12})$$

Here  $p_a$  is the air pressure,  $\zeta$  is the elevation of the free surface and  $H$  is the water depth;  $q_T$  and  $q_S$  are the heat and salt fluxes, respectively.

The kinematic boundary condition A12 signifies that a fluid particle at the surface remains there regardless of possible advective motion of the underlying layers.

At the sea-bed  $z = H(x,y)$  the boundary conditions are:

$$u = v = w = 0, \quad (\text{A13})$$

$$\vartheta_T \frac{\partial T}{\partial z} = \vartheta_S \frac{\partial S}{\partial z} = 0. \quad (\text{A14})$$

The bottom stress is taken into account in the form of a quadratic law (Blumberg and Mellor 1987). The solid vertical walls are taken to be of the no-slip type. Neither these nor the seabed are permeable for the scalar properties, excepting the locations where rivers discharge. At these points the salinity is prescribed as zero, and the river water is assumed to adapt instantaneously to the ambient temperature. For the entire Baltic model, a passive radiation condition for the surface elevation (Mutzke 1998, Orlanski 1976), combined with a sponge-layer approach for other variables, is used. For the Gulf model the combination of an active radiation condition with a sponge-layer approach is used for all variables. A sponge layer is defined as the zone adjacent to an open boundary where the lateral diffusivity coefficient increases linearly towards the open boundary. In our calculations the width of this zone was taken to be 9 grid cells; the increment of the lateral diffusivity coefficient was prescribed as 10 and 5  $\text{m}^2 \text{s}^{-1}$  for the coarse and fine models, respectively.

## Numerical scheme

Since a comprehensive description of the numerical scheme has been given by Andrejev and Sokolov (1989, 1990) and Sokolov *et al.* (1997), only a brief outline of its main features is provided here. The governing equations are used in flux form to ensure that a number of integral constraints (Blumberg and Mellor 1987) are maintained. The finite-difference approximations are constructed by integrating the model equations over the C-grid cell volume (Mesinger and Arakawa 1976). The time step was split up, as suggested by Liu and Leendertse (1978), and thus the  $u$ -equations are solved at time steps  $n - 1/2 \sim n + 1/2$ , the  $v$ -equations are solved at time steps  $n \sim n + 1$ , and all other equations are solved at every half time step. All vertical derivatives as well as the bottom friction were treated implicitly. The mode-splitting technique (Simons 1974) was employed, where the two-dimensional equation for the volume transport (*viz.* the external mode) was obtained by vertical summation of the finite-difference approximations of the three-dimensional momentum equations. Before the three-dimensional finite-difference equations corresponding to the internal mode can be resolved, the sea-surface elevation must be calculated from the volume transport equation and from the vertically-integrated equation of continuity. The frictional stress at the bottom enters semi-implicitly into both modes and is based on a bottom-layer velocity, which is calculated using an iterative procedure. The two- and three-dimensional momentum equations are thus solved repeatedly until the absolute value of the maximum difference between the bottom velocities for subsequent iterations becomes smaller than an *a priori* prescribed very small positive number. This adjustment process permits the use of an alternating-direction implicit method for solving the volume transport equation (Liu and Leendertse 1978, Andrejev and Sokolov 1989), and furthermore allows the use of the same time step (in the present study 1 hour) for the two- as well as the three-dimensional elements of the model. The Gaussian elimination method makes it possible to solve these equations quite easily.